Histol Histopathol (2009) 24: 141-148

http://www.hh.um.es

Histology and Histopathology

Cellular and Molecular Biology

Tracing the accumulation and effects of mercury uptake in the previtellogenic ovary of crucian carp, *Carassius auratus gibelio* by autometallography and caspase-3 immunohistochemistry

Otilia Zarnescu

Department of Animal Biology, Faculty of Biology, University of Bucharest, Bucharest, Romania

Summary. The aims of the present study were to apply the AMG technique for localization of mercury at the light and electron microscopic level in the ovary of crucian carp after exposure to mercuric chloride and to find out if this heavy metal induces expression of caspase-3. Depending on the stage of ovarian follicle development, two patterns of mercury accumulation have been found in previtellogenic ovary of crucian carp. The first mercury accumulation pattern has been found in the early previtellogenic oocyte without zona radiata. In these oocytes, mercury accumulates into an ooplasmic region that seems to correspond to the Balbiani body (32-65 µm oocyte diameter), throughout the cytoplasm (84-116 µm oocyte diameter) and in the cortical cytoplasm (~180 µm oocyte diameter). The second mercury accumulation pattern has been found in the late previtellogenic oocyte with cortical alveoli (229-330 µm oocyte diameter). Ultrastructural observations have shown grains of silver-enhanced mercury inside coated vesicles, the cortical lysosome-like bodies or multivesicular bodies and cortical alveoli. Immunohistochemistry reaction for caspase-3 was positive in nuclei of the early previtellogenic oocyte and Balbiani body.

Key words: Autometallography, Mercuric chloride, Ultrastructure, Caspase-3, Fish

Introduction

Mercury contamination of water, both fresh and saltwater, through natural and man-made sources is a major problem due to the ability of fish to accumulate mercury in their tissues (Gwaltney-Brant, 2002). Mercury accumulation in fish has been studied mostly by quantitative methods which gave information on retention and elimination of the metal from different organs under various experimental conditions. Studies of histochemical localization of mercury in fish are scarce. On the other hand, subcellular accumulations of mercury have not been available until the introduction of autometallography (AMG) for tracing mercury accumulations (Timm, 1962; Danscher, 1984; Danscher and Moller-Madsen, 1985; Stoltenberg and Danscher, 2000). So far, AMG has been performed on fish tissues only to demonstrate mercury in kidney and liver of rainbow trout (Baatrup et al., 1986; Baatrup and Danscher, 1987) and in salmon olfactory system (Baatrup and Døving, 1990), endogenous zinc in rainbow trout (Baatrup, 1989), copper in tilapia gills (Dang et al., 1999) and cadmium in liver of turbot (Amaral et al., 2002). To date, only one AMG study has been done on fish ovary, but it was performed only at the light microscope level (Mester and Zarnescu, 1996).

Apoptosis has been demonstrated in the ovary of several fish species, including goldfish and rainbow trout, both *in vivo* and *in vitro* (Janz and Van der Kraak, 1997; Wood and Van der Kraak, 2001) and fathead minnows after exposure to dietary methylmercury (Drevnick et al., 2006). Molecular components associated with apoptosis, including effector caspases, such as caspase-3, have been shown to be present in the ovary of mammals, birds (reviewed in Habibi and Andreu-Vieyra, 2007) and fish (Andreu-Vieyra et al., 2005). In addition, studies in the mammalian systems have demonstrated that the exposure of cultured cells to mercuric chloride led to cell death, and caspase-3 activation (Sutton and Tchounwou, 2006; Park and Park, 2007).

The aims of the present study were to apply the AMG technique for localization of mercury at the light and electron microscopic level in the ovary of crucian carp after exposure to mercuric chloride and to find out

Offprint requests to: Otilia Zarnescu, Department of Animal Biology, Faculty of Biology, University of Bucharest, Splaiul Independentei 91-95, Bucharest-5, R-050095, Romania. e-mail: otilia@bio.unibuc.ro

if this heavy metal induces expression of caspase-3.

Material and methods

Animals

Female crucian carp, *Carassius auratus gibelio*, weighing between 30 and 40 g were purchased from the Fisheries Farm Nucet. The specimens were acclimatized to laboratory conditions for two weeks, at room temperature in glass aquaria, containing tap water.

Mercury exposure

Two groups of fish were intraperitoneally (IP) injected with $HgCl_2$ dissolved in a saline solution isotonic for freshwater teleost. Fishes from first group were injected with 500 µg $HgCl_2$ and sacrificed at 2, 3, 7 and 24 hours and 2 days after injection. The second group received two injections, first with 500 µg $HgCl_2$ and second with 250 µg $HgCl_2$. The second injection was done three days after first injection. These fishes were sacrificed at 4, and 7 days after first injection. Five fish were kept in clean freshwater, serving as controls.

Light microscope autometallography

Fragments of crucian carp ovary were fixed in Bouin solution with 2% DMSO, dehydrated in ethanol, cleared in toluene and embedded in paraffin. Paraffin sections were silver-enhanced for microscopic analysis following the autometallographic method of Danscher (1984) and Danscher and Møller-Madsen (1985). Briefly, paraffin sections (5 µm) were incubated 1 h, at 26°C, in the dark, in AMG solution: 60 ml gum arabic (25%); 10 ml sodium citrate buffer (0.80 M sodium citrate in 1.27 M citric acid); 15 ml reducing agent (0.51 M hydroquinone); 15 ml silver ion supply (0.03 M silver lactate). All solutions were prepared with deionized water. After development, the sections were washed in running tap water at 40°C for 40 min and then incubated for 12 min in 5% sodium thiosulfate. The sections were stained with 1% neutral red and examined with an Zeiss Axiostar Plus microscope (Zeiss). The photomicrographs were taken by digital camera (AxioCam MRc 5, Carl Zeiss) driven by software AxioVision 4.6 (Carl Zeiss).

Ultrastructural autometallography

Small ovary fragments were fixed in 2.5% glutaraldehide, buffered at pH 7.4 in 0.1M sodium cacodylate, then post-fixed in 1% OsO_4, in the same cacodylate buffer, dehydrated and embedded in Epon 812. Ultrastructural autometallography was performed by direct development of the ultrathin sections (Danscher, 1984). Ultrathin sections were placed on 200-mesh Formvar-coated nickel grids. After being dipped in a 0.5% gelatin solution each grid was placed on a drop of AMG developer without gum arabic, 2-9 min, in the dark. After AMG development, the grids were sequentially incubated in 20% sodium thiosulfate (2 min) and deionized water (5 min). Ultrathin sections were stained with uranyl acetate and lead citrate, and then studied with a 208S Phillips/FEI electron microscope operating at 80 KV.

Immunohistochemistry

7 µm-thick paraffin sections were sequentially incubated in 3% H_2O_2 to remove endogenous peroxidase (10 min), washed in phosphate-buffered saline (PBS) and incubated with 2% bovine serum albumin (BSA, fraction V) to block non-specific background staining (30 min). Tissue sections were incubated overnight, at 4°C with rabbit anti caspase-3 polyclonal antibody (USBiological), diluted 1:100, rinsed with PBS then followed by the incubation with secondary goat anti rabbit IgG peroxidase conjugate (Rockland) diluted 1:1250, 1 h, at room temperature. Each incubation step was followed by four 5 min rinses in PBS. To visualize the primary antibody binding sites, the sections were incubated for 5-15 min in a solution of 0.05% 3.3'-diaminobenzidine tetrachloride (DAB) and 0.015% hydrogen peroxide, dissolved in PBS. As a negative control of immunohistochemical reaction, sections were processed as described above except that the primary antibody was omitted.

Results

After the autometallographic development, the mercury deposits (made visible by the silver grains) were seen only in the sections from fishes injected with mercuric chloride and not in the control (non-injected) animals.

The ovary of fish used in the experiment was characterized by the presence of early and late previtellogenic follicles with cortical alveoli. Cortical alveoli make their first appearance in the peripheral ooplasm. By the end of previtellogenic stage, cortical alveoli fill almost the entire oocyte cytoplasm, but in the subsequent stages they continue to form and are displaced at the periphery of the oocyte by yolk proteins which accumulate centripetally. In the oocyte of crucian carp, the cortical alveoli consists of colloidal material and a spherical body. The zona radiata appears coincident with cortical alveoli and is first observed as a thin band between the oocyte and the overlying granulosa cells.

Mercury begins to accumulate in the cytoplasm of previtellogenic oocytes approximately three hours after IP injection. Depending on stage of ovarian follicle development, two patterns of mercury accumulation have been found in previtellogenic ovary of crucian carp. The first mercury accumulation pattern has been found in the early previtellogenic oocytes without zona radiata. In these oocytes, mercury accumulates in an ooplasmic region that seems to correspond to Balbiani body (32-65 µm oocyte diameter) (Fig. 1A), throughout the cytoplasm (84-116 µm oocyte diameter) (Fig. 1B)

and in the cortical cytoplasm (~180 µm oocyte diameter). Moreover, in some early previtellogenic oocyte silver-enhanced mercury has been found as juxtanuclear aggregates (Fig. 1B). At this point we can only speculate on the identity of these mercury accumulations as being multivesicular bodies associated to Balbiani body. Localization of mercury in these primary growth stage oocytes have been confirmed by the ultrastructural AMG (Fig. 1C-D).

The second mercury accumulation pattern has been found in the late previtellogenic oocyte with cortical alveoli (229-330 µm oocyte diameter). In these oocytes mercury enters ovarian follicles through capillaries of the theca layer, reaches the granulosa layer and has contact with the oocyte surface through the pore canals of the zona radiata (Fig. 2A). Ultrastructural observations have shown grains of silver-enhanced mercury inside coated vesicles (Fig. 2B) and in the

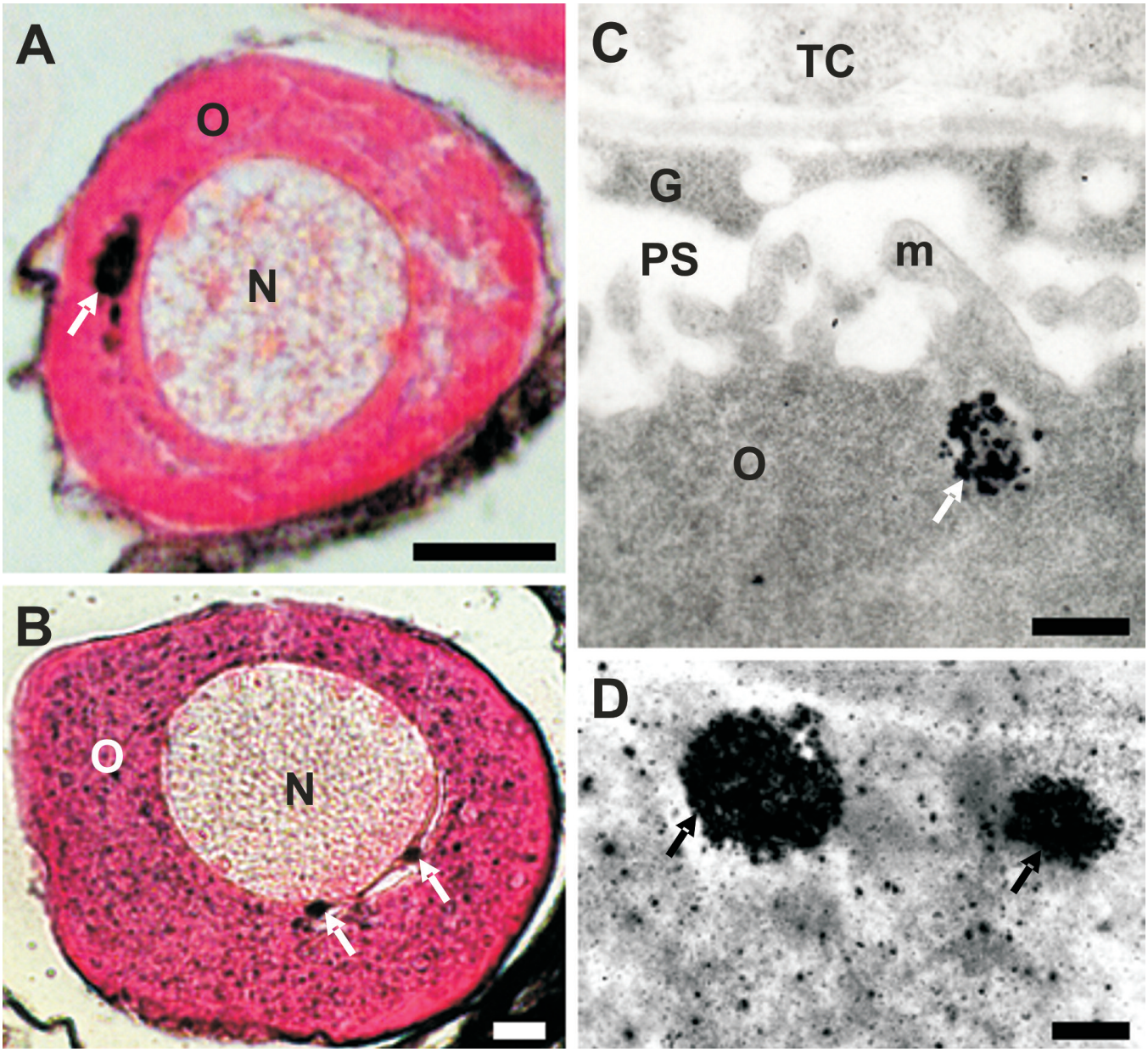

Fig. 1. A. AMG localization of mercury in the early previtellogenic oocyte. A Mercury deposits were found in the Balbiani body (arrow) of 32-65 µm oocyte diameter (seven days after mercury injection). **B.** The ooplasm of 84-116 µm oocyte diameter contains a large amount of AMG grains at seven days after IP injection. Note the accumulation of silver-enhanced mercury in the juxtanuclear aggregates (arrows). Electron micrograph of silver-enhanced mercury (arrow) located in the multivesicular body from cortical ooplasm **(C)** and throughout cytoplasm **(D)** of oocytes at three hours after IP injection. G: granulosa cell; m: microvillus; N: nucleus; O: ooplasm; PS: perivitelline space; TC: theca cells. Scale bars: a, b, 10 µm; c, 1 µm; d, 0.5 µm.

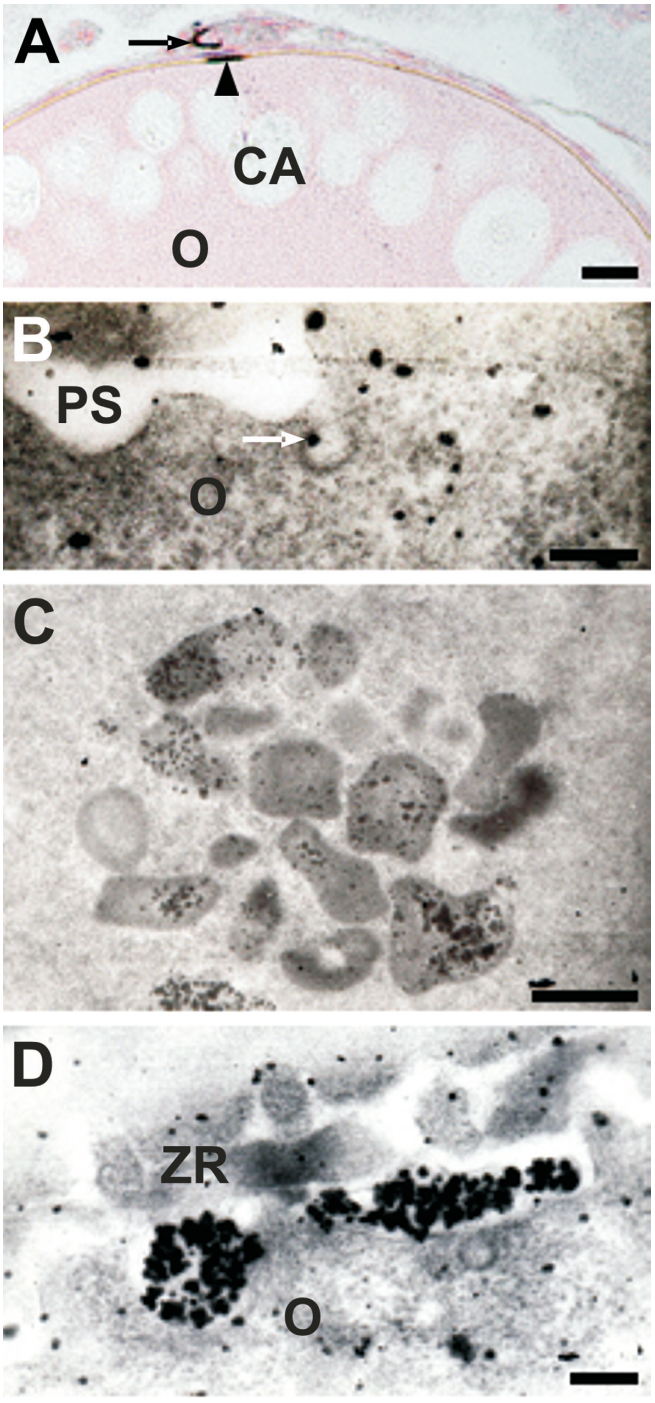

Fig. 2. AMG localization of mercury in the late previtellogenic oocyte. **A.** AMG visualization of mercury transfer from capillaries of the theca interna (arrow) to zona radiata (arrowhead). Electron micrograph of silver enhanced mercury inside coated vesicles (arrow; **B**) and lysosome-like bodies **(C)** at two hours after IP injection. **D.** Electron micrograph of abundant AMG staining in the perivitelline space at seven days after IP injection. CA: cortical alveoli; O: ooplasm; PS: perivitelline space; ZR: zona radiata. Scale bar: a, 20 µm; b, 0.2 µm; c, 1 µm; d, 0.3 µm.

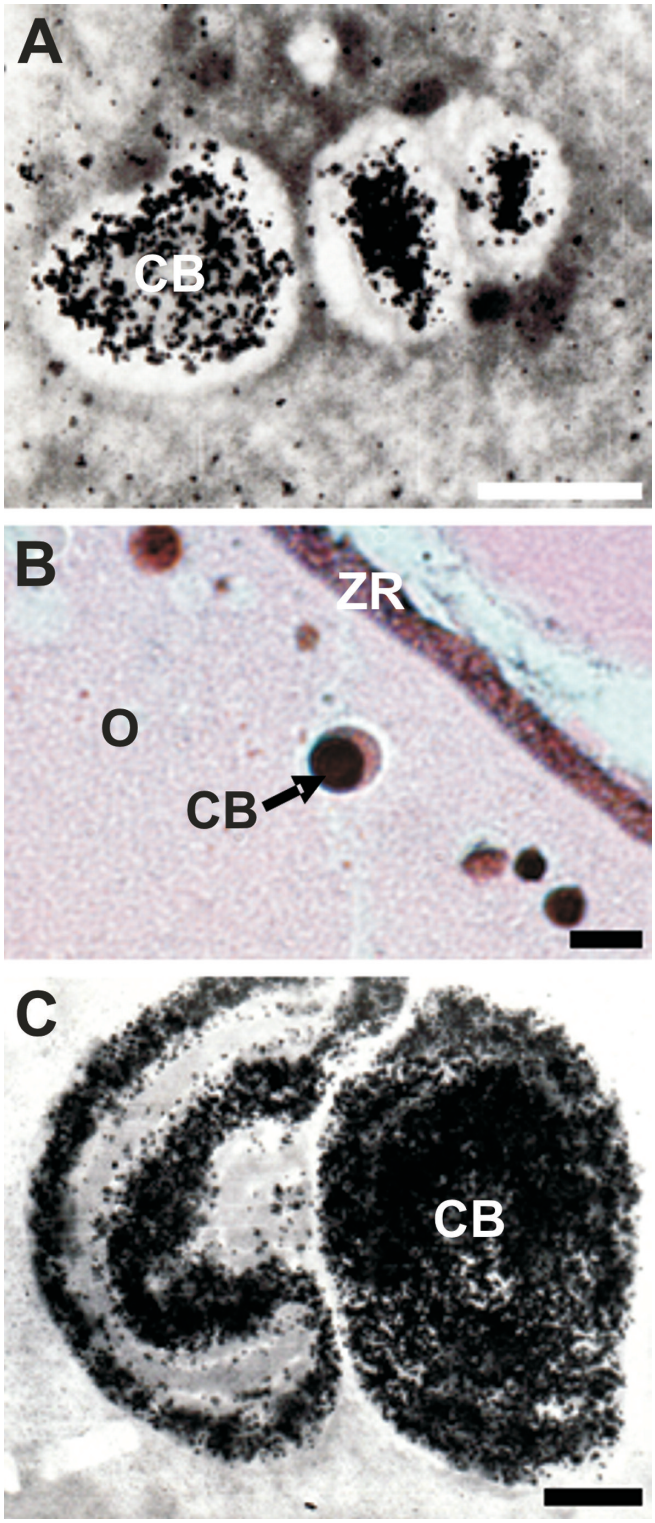

Fig. 3. AMG localization of mercury in the cortical alveoli. **A.** Electron micrograph showing mercury accumulation in the nascent cortical alveoli at 24 hours after IP injection. Light **(B)** and electron **(C)** micrograph of mercury deposits in the central spherical body (CB) of the cortical alveoli at two days after IP injection. O: ooplasm; ZR: zona radiata. Scale bar: a, c, 1 µm; b, 10 µm.

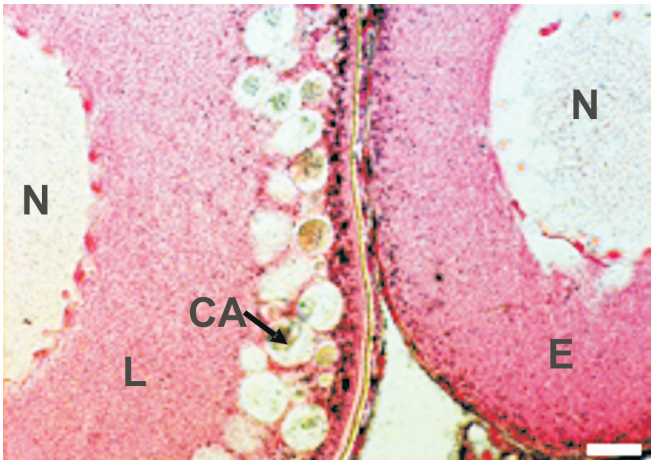

Fig. 4. AMG localization of mercury in the cortical cytoplasm of early (E) and late (L) previtellogenic oocytes, at four days after IP injection. CA: cortical alveoli; N: nucleus. Scale bar: 20 µm.

cortical lysosome-like body (Fig. 2C). At seven days after IP injections in the perivitelline space intense accumulation of silver-enhanced mercury was present (Fig. 2D). At the beginning of cortical alveolus stage, mercury starts to accumulate in the central spherical body of the nascent cortical alveoli (Fig. 3A). In both light (Fig. 3B) and electron (Fig. 3C) microscopy the highest density of silver-enhanced mercury was found within the central spherical body of cortical alveoli and cortical cytoplasm. Interestingly, by the end of cortical alveolus stage there is little or no accumulation of mercury in the spherical body of the cortical alveoli. In this stage mercury taken up by the oocyte accumulated mainly in the cortical ooplasm (Fig. 4).

Immunohistochemistry reaction for caspase-3 was mostly positive in nuclei of the early previtellogenic oocyte at three hours after IP injection (Fig. 5A). The number of caspase-3 positive nuclei increased with time, reaching a maximum, at 24 hours after mercury injection. Moreover, in some early previtellogenic oocytes, positive staining was also detected in the ooplasm, in an ooplasmic region that seems to correspond to the Balbiani body (Fig. 5B,C). Furthermore, immunoreactivity for caspase-3 was not detectable, nor in the ovary of the control fishes neither in the control sections incubated with PBS instead of primary antibody (data not shown).

Discussion

As far as we know this is the first report describing the use of AMG at the electron microscope level for tracing mercury accumulation in fish oocytes. Moreover, up to date, caspase-3-like activity has been detected in cultured atretic follicles of *Oncorhynchus mykiss* (Wood and Van der Kraak, 2003), gonadal differentiation of the *Sparus aurata* (Soverchia et al., 2007) and in the follicular layer of the postovulatory follicles of the *Prochilodus argenteus* (Santos et al., 2008). No work has been found about caspase-3 immunohistochemistry in fish oocytes.

In our study mercury begins to accumulate in the cytoplasm of previtellogenic oocytes approximately three hours after IP injection. In a quantitative study (Weisbart, 1973) also reported that the ovary of goldfish manifested the highest levels of $^{203}Hg(NO_3)_2$ at three hours and eight days after IP injections.

Our electron microscope findings demonstrate that mercury was accumulated within the coated vesicle of late previtellogenic follicle, probably bound to vitellogenin (VTG). VTG is the principal precursor to yolk protein in oviparous vertebrates (Babin et al., 2007). This lipoglycophospholipoprotein is produced in the liver and released into the blood-stream, sequestered by developing oocyte and proteolytically cleaved (Lange, 1985). The proteolitic products are stored as yolk. The VTG molecule itself may be implicated in the transport of hepatic heavy metals to gonad, due to its protein phosphorus-dependent charge and ion binding capacity (Hara et al., 1980). Very little is currently known about the specific mechanisms involved in the cellular uptake and transport of inorganic mercury. Once inorganic mercury is introduced into the blood, a significant fraction of mercury enters and/or is bound to cellular components of blood. The remainder binds to various ligands in plasma, most of which possess one or more free sulphydryl groups with which the mercury can bind. In the sockeye and coho salmon, inorganic mercury or methylmercury are incorporated in lipoproteins and their interaction with salts of heavy metals changes the surface structure of lipoprotein (Reichert and Malins, 1974). Since in our previous work we found mercury in the yolk platelets (Mester and Zarnescu, 1996) we can assume that mercury could enter in the oocytes bound to VTG.

Another finding in this study was accumulation of mercury in the central spherical body of the cortical alveoli. The cortical alveoli in the oocytes of some freshwater teleosts are composed of a polysaccharide-protein complex (Donato et al., 1980); their protein content being rich in cysteine and tyrosine, whereas the polysaccharide content consists of chondroitin sulphate-, and traces of polygalacturonic acid. Synthesis of the cortical alveoli occurs at the beginning of yolk accumulation, when the internatization of VTG is discrete (Perazzolo et al., 1999). It has been established that mercury bound to endogenous sulphide serves as a catalytic center for the reduction of silver ions to metallic silver (Danscher, 1984). Accumulation of metals (gold) was also demonstrated ultrastructurally, in the cortical alveoli from ovaries of rats injected IP with sodium aurothiomalate (Møller-Madsen et al., 1985).

Intracellulary, mercury was found predominantly in the lysosome, multivesicular bodies, vacuoles and cytoplasm. The chemical form of the lysosomal accumulations of mercury has been assumed to be

mercury sulphyde polymers (Danscher and Schroder, 1979).

In the present study, immunohistochemistry has revealed the presence of caspase-3 in the nuclei of early previtellogenic oocytes. Caspase-3 is an effector caspase that initiates degradation of the cell in the final stages of apoptosis and is synthesized as a latent proenzyme. In response to various death signals, the caspase-3 proenzyme is cleaved by initiator caspases to generate the active large (p17) and small (p12) subunits, forming an active heterotetramer (Woo et al., 1998; Zheng et al., 1998). Although it has been widely accepted that procaspase-3 is cleaved to generate the active form in the cytoplasm, the enzymatic activity of capase-3-like proteases can be found in the nuclear fraction of apoptotic cells (Martins et al., 1997; Mandal et al., 1999;

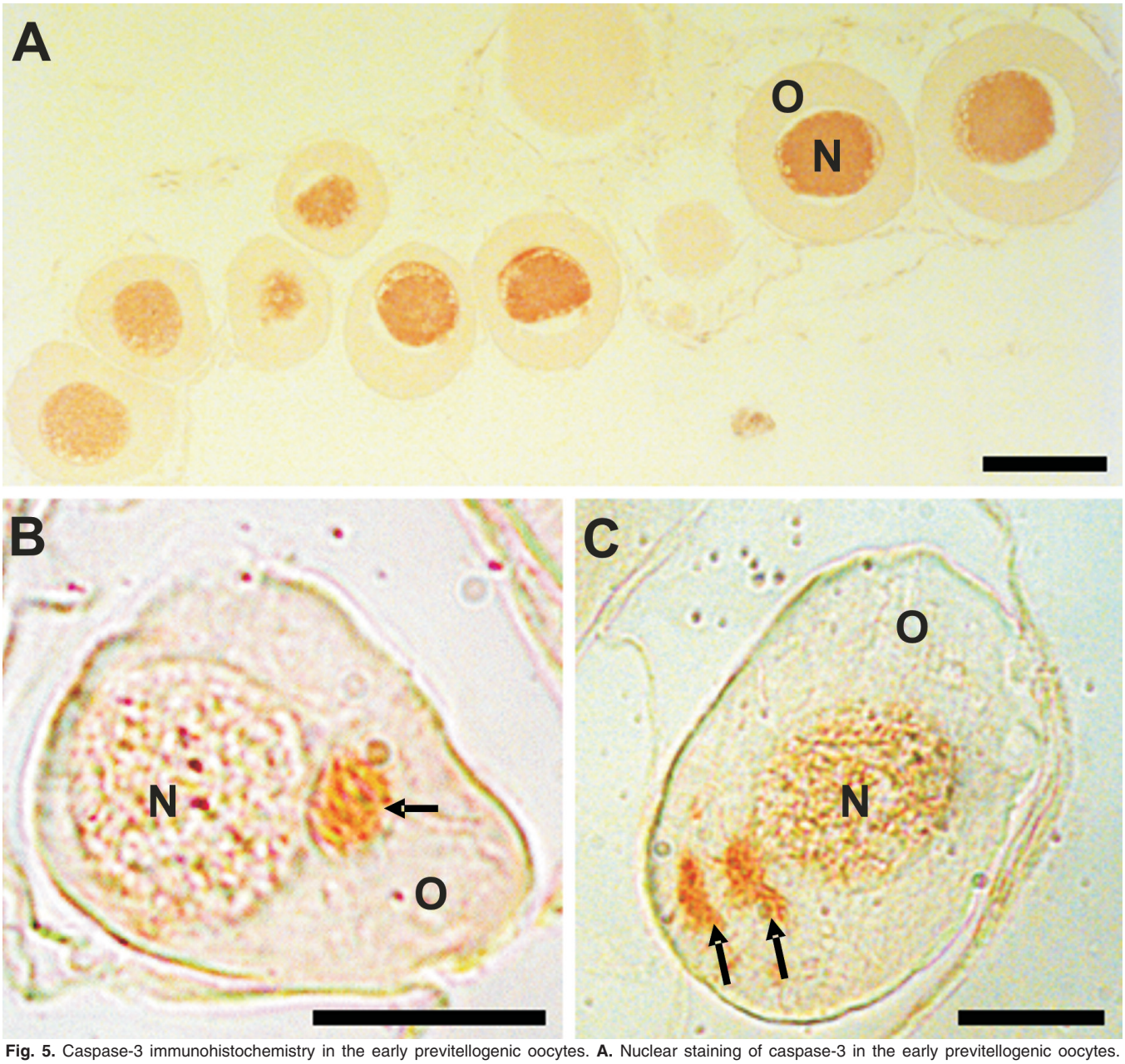

Fig. 5. Caspase-3 immunohistochemistry in the early previtellogenic oocytes. **A.** Nuclear staining of caspase-3 in the early previtellogenic oocytes. Immunohistochemical localization of caspase 3 in the Balbiani body (arrow) of 33.85 µm oocyte diameter **(B)** and 64.51 µm oocyte diameter **(C).** N: nucleus; O: ooplasm. No positive reactions were seen in the control sections incubated with 2% BSA in PBS instead of primary antibody (data not shown). Scale bars: a, 100 µm; b, c, 20 µm.

Takemoto et al., 2003; Kamada et al., 2005). In this regard, a recent immunohistochemical study has shown the presence of active caspase-3 in nucleus of oocytes from rat atretic pre-antral follicles (Ortiz et al., 2006). Several studies have provided evidence that in mammalian cell cultures mercury induces activation of caspase-3 (Lee et al., 2006; Sutton and Tchounwou, 2006). In the light of the findings of our study, we can therefore reasonably speculate that the presence of immunostaining for caspase-3 in the nucleus of the early previtellogenic oocytes might indicate apoptosis of these oocytes as a consequence of mercury exposure.

The data of the present study indicates that in the early previtellogenic oocytes both caspase-3 and mercury were localized in the region of the Balbiani body. Few studies on caspase-3 distribution in fish ovary have been reported (reviewed in Habibi and Andreu-Vieyra, 2007). On the other hand, in the *Xenopus* oocytes, pro-and antiapoptotic proteins are located in distinct subcellular compartments, with proapoptotic proteins Bax and p53 being sequestered in the oocyte nucleus and antiapoptotic protein Bcl-x_L sequestered in the cytoplasm and highly enriched in the mitochondrial cloud (Kloc et al., 2007). In most teleost fish, the Balbiani body is a prominent feature of previtellogenic oocytes and although it morphology is highly variable, even between closely related fish species, it usually contains a nuage, mitochondria, multivesicular bodies, endoplasmic reticulum, and Golgi complexes (Zelazowska et al., 2007). Because the antibody used in this study can recognize both the inactive and active forms of caspase-3 we can assume that nuclear immunostaining reflects active caspase-3, while cytoplasmic immunostaining may be associated with active/inactive caspase-3.

In conclusion, the results of this study demonstrate a stage-dependent accumulation of mercury in the previtellogenic oocytes of crucian carp and suggest that mercury can be implicated in activation of caspase-3 and oocyte apoptosis. Further analysis needs to be done to confirm the obtained preliminary data and to evaluate the role of apoptotic proteins in the fish ovary.

References

Amaral A.F., Alvarado N., Marigomez I., Cunha R., Hylland K. and Soto M. (2002). Autometallography and metallothionein immunohistochemistry in hepatocytes of turbot (*Scophthalmus maximus* L.) after exposure to cadmium and depuration treatment. Biomarkers 7, 491-500.

Andreu-Vieyra C.V., Buret A.G. and Habibi H.R. (2005). Gonadotropin-releasing hormone induction of apoptosis in the testes of goldfish (*Carassius auratus*). Endocrinology 146,1588-1596.

Baatrup E. (1989). Selenium-induced autometallographic demonstration of endogenous zinc in organs of the rainbow trout, *Salmo gairdneri*. Histochemistry 90, 417-425.

Baatrup E. and Danscher G. (1987). Cytochemical demonstration of mercury deposits in trout liver and kidney following methyl mercury intoxication: differentiation of two mercury pools by selenium. Ecotoxicol. Environ. Saf. 14,129-141.

Baatrup E. and Døving K.B. (1990). Histochemical demonstration of mercury in the olfactory system of salmon (*Salmo salar* L.) following treatments with dietary methylmercuric chloride and dissolved mercuric chloride. Ecotoxicol. Environ. Saf . 20, 277-289.

Baatrup E., Nielsen M.G. and Danscher G. (1986). Histochemical demonstration of two mercury pools in trout tissues: mercury in kidney and liver after mercuric chloride exposure. Ecotoxicol. Environ. Saf. 12, 267-282.

Babin P.J., Carnevali O., Lubzens E. and Schneider W.J. (2007). Molecular aspects of oocyte vitellogenesis in fish. In: The fish oocyte from basic studies to biotechnological applications. Babin P.J., Cerdà J. and Lubzens E. (eds) Springer. The Netherlands, pp 39-76.

Dang Z., Lock R.A., Flik G. and Wendlelaar Bonga S.E. (1999). Metallothionein response in gills of *Oreochromis mossambicus* exposed to copper in fresh water. Am. J. Physiol. 277, R320-R331.

Danscher G. (1984). Autometallography. A new technique for light and electron microscopic visualization of metals in biological tissues (gold, silver, metal sulphides and metal selenides). Histochemistry 81, 331-335.

Danscher G. and Møller-Madsen B. (1985). Silver amplification of mercury sulfide and selenide: a histochemical method for light and electron microscopic localization of mercury in tissue. J. Histochem. Cytochem. 33, 219-228.

Danscher G. and Schrøder H.D. (1979). Histochemical demonstration of mercury induced changes in rat neurons. Histochemistry 60, 1-7.

Donato A., Contini A., Maugeri A. and Fasulo S. (1980). Structural and ultrastructural aspects of the growing oocytes of *Chromis chromis* (Teleostei, Labridae). Riv. Biol. Norm. Pathol. 6, 31-66.

Drevnick P.E., Sandheinrich M.B. and Oris J.T. (2006). Increased ovarian follicular apoptosis in fathead minnows (*Pimephales promelas*) exposed to dietary methylmercury. Aquat. Toxicol. 79, 49-54.

Gwaltney-Brant S.M. (2002). Heavy metals. In: Handbook of toxicologic pathology. 2nd ed. Haschek W.M., Rousseaux C.G. and Wallig M.A. (eds). Academic Press. pp 701-733.

Habibi H.R. and Andreu-Vieyra C.V. (2007). Hormonal regulation of follicular atresia in teleost fish. In: The fish oocyte from basic studies to biotechnological applications. Babin P.J., Cerdà J. and Lubzens E. (eds). Springer. The Netherlands. pp 235-253.

Hara A., Yamauchi K. and Hirai H. (1980). Studies on female-specific serum protein (vitellogenin) and egg yolk protein in Japanese eel (*Anguilla japonica*). Comp. Biochem. Physiol. 65B, 315-320.

Janz D.M. and van der Kraak G. (1997). Suppression of apoptosis by gonadotropin, 17beta-estradiol, and epidermal growth factor in rainbow trout preovulatory ovarian follicles. Gen. Comp. Endocrinol. 105, 186-193.

Kamada S., Kikkawa U., Tsujimoto Y. and Hunter T. (2005). Nuclear translocation of caspase-3 is dependent on its proteolytic activation and recognition of a substrate-like protein(s). J. Biol. Chem. 280, 857-860.

Kloc M., Shirato Y., Bilinski S., Browder L.W. and Johnston J. (2007). Differential subcellular sequestration of proapoptotic and antiapoptotic proteins and colocalization of Bcl-x(L) with the germ plasm, in *Xenopus laevis* oocytes. Genesis 45, 523-531.

Lange R.H. (1985). The vertebrate yolk-platelet crystal: Comparative analysis of an in vitro crystalline aggregate. Int. Rev. Cytol. 97, 133-181.

Lee J.H., Youm J.H. and Kwon K.S. (2006). Mercuric chloride induces

apoptosis in MDCK cells. J. Prev. Med. Pub. Health. 39, 199-204. [Article in Korean].

Mandal M., Adam L. and Kumar R. (1999). Redistribution of activated caspase-3 to the nucleus during butyric acid-induced apoptosis Biochem. Biophys. Res. Commun. 260, 775–780.

Martins L.M., Mesner P.W., Kottke T.J., Basi G.S., Sinha S., Tung J.S., Svingen P.A., Madden B.J., Takahashi A., McCormick D.J., Earnshaw W.C. and Kaufmann S.H. (1997). Comparison of caspase activation and subcellular localization in HL-60 and K562 cells undergoing etoposide-induced apoptosis. Blood 90, 4283-4296.

Mester R. and Zarnescu O. (1996). Histochemical localization of mercury in the ovary of crucian carp, *Carassius auratus gibelio*, after exposure to mercuric chloride. Rev. Roumaine Biol. Ser. Biol. Anim 41, 25-34.

Møller-Madsen B., Simonsen O.H., Doss D.N. and Danscher G. (1985). Gold in the ovary of rats exposed to sodium aurothiomalate. Exp. Mol. Pathol. 42, 287-292.

Ortiz R., Echeverría O.M., Salgado R., Escobar M.L. and Vázquez-Nin G.H. (2006). Fine structural and cytochemical analysis of the processes of cell death of oocytes in atretic follicles in new born and prepubertal rats. Apoptosis 11, 25-37.

Park E.J. and Park K. (2007). Induction of reactie oxygen species and apoptosis in BEAS-2B cells by mercuric chloride. Toxicol. In Vitro 21, 789-794.

Perazzolo L.M., Coward K., Davail B., Normand E., Tyler C.R., Pakdel F., Schneider W.J. and Le Menn F. (1999). Expression and localization of messenger ribonucleic acid for the vitellogenin receptor in ovarian follicles throughout oogenesis in the rainbow trout, *Oncorhynchus mykiss*. Biol. Reprod. 60, 1057-1068.

Reichert W.L. and Malins D.C. (1974). Interaction of mercurials with salmon serum lipoproteins. Nature 247, 569-570.

Santos H.B, Sato Y., Moro L., Bazzoli N. and Rizzo E. (2008). Relationship among follicular apoptosis, integrin beta1 and collagen type IV during early ovarian regression in the teleost Prochilodus argenteus after induced spawning. Cell Tissue Res. 332, 159-170.

Soverchia L., Carotti M., Andreu-Vieyra C., Mosconi G., Cannella N., Habibi H. and Polzonetti-Magni A.M. (2007). Role of gonadotropin-releasing hormone (GnRH) in the regulation of gonadal differentiation in the gilthead seabream (*Sparus aurata)*. Mol. Reprod. Dev. 74, 57-67.

Stoltenberg M. and Danscher G. (2000). Histochemical differentiation of autometallographically traceable metals (Au, Ag, Hg, Bi, Zn): protocols for chemical removal of separate autometallographic metal clusters in Epon sections. Histochem. J. 32, 645-652.

Sutton D.J. and Tchounwou P.B. (2006). Mercury-induced externalization of phosphatidylserine and caspase 3 activation in human liver carcinoma (HepG2) cells. Int. J. Environ. Res. Public Health. 3, 38-42.

Takemoto K., Nagai T., Miyawaki A. and Miura M. (2003). Spatio-temporal activation of caspase revealed by indicator that is insensitive to environmental effects. J. Cell Biol. 160, 235–243.

Timm F. (1962). Histochemische lokalisation und nachweis der schwermetalle. Acta Histochem. Suppl. 3 46, 706-711.

Weisbart M. (1973). The distribution and tissue retention of mercury-203 in the goldfish (*Carassius auratus*). Can. J. Zool. 119, 405-433.

Woo M., Hakem R., Soengas M.S., Duncan G.S., Shahinian A., Kagi D., Hakem A., McCurrach M., Khoo W., Kaufman S.A., Senaldi G., Howard T., Lowe S.W. and Mak T. W. (1998). Essential contribution of caspase 3/CPP32 to apoptosis and its associated nuclear changes. Genes Dev. 12, 806-819.

Wood A.W. and Kraak G. van der. (2001). Apoptosis and ovarian function: novel perspectives from the teleosts. Biol. Reprod. 64, 264-271.

Wood A.W. and van der Kraak G. (2003). Yolk proteolysis in rainbow trout oocytes after serum-free culture: evidence for a novel biochemical mechanism of atresia in oviparous vertebrates. Mol. Reprod. Dev. 65, 219-227.

Zelazowska M., Kilarski W., Bilinski S.M., Podder D.D. and Kloc M. (2007). Balbiani cytoplasm in oocytes of a primitive fish, the sturgeon Acipenser gueldenstaedtii, and its potential homology to the Balbiani body (mitochondrial cloud) of *Xenopus laevis* oocytes. Cell Tissue Res. 329, 137-145.

Zheng T.S., Schlosser S.F., Dao T., Hingorani R., Crispe I.N., Boyer J.L. and Flavell R.A. (1998). Caspase-3 controls both cytoplasmic and nuclear events associated with Fas-mediated apoptosis in vivo. Proc. Natl. Acad. Sci. USA 95, 13618–13623.

Accepted August 12, 2008